Mater. Res. Soc. Symp. Proc. Vol. 1019 © 2007 Materials Research Society 1019-FF06-04

Cell Response and Tissue Scaffold Triggers Investigated by Scanning Probe Recognition Microscopy

Q. Chen[1], Y. Fan[1], S. Kumar[1], A. D. Baczewski[1], L. Udpa[1], V. M. Ayres[1], I. Ahmed[2], S. Meiners[2], and A. F. Rice[3]
[1]Michigan State University, East Lansing, MI, 48824
[2]UMDNJ-Robert Wood Johnson Medical School, Piscataway, NJ, 08854
[3]Veeco Metrology Group, Santa Barbara, CA, 93117

ABSTRACT

Recent efforts in the field of regenerative medicine have focused on the fabrication of scaffolds capable of promoting a repertoire of cellular responses. These scaffolds are designed to be mimetic in structure and function to the extracellular matrix/basement membrane, which serves as the physiological support for cells within tissues. Understanding the nature of the physical interactions of cells within these biomimetic structures and deriving information that would correlate geometric properties of the scaffolds with the promotion of specific cellular responses would have a major impact on their design and utility. In this paper, we introduce the use of a new and powerful form of atomic force microscopy developed by our group, termed Scanning Probe Recognition Microscopy (SPRM). SPRM is used to examine the physical interactions of protrusions emanating from NIH 3T3 fibroblasts with the surfaces of both 2D planar and 3D nanofibrillar cell culture surfaces. This technique provides the means to maintain focus on user defined regions of contact (in the nanometer range) between the cell protrusions and the 2D and 3D surfaces. Differences in the number and shape of contact regions between the cell protrusions and the two types of surface were observed using SPRM. These observations were supported by similar imaging results obtained, albeit at significantly lower resolution, using phase contrast and bright field microscopy.

INTRODUCTION

The use of scaffolds composed of biocompatible materials as vehicles to deliver or promote growth/differentiation of cells within damaged tissues of the body is an exciting new tool for the field of regenerative medicine. To optimize the performance of these scaffolds for each type of tissue or application, new analytical methods must be developed that can examine the interaction of these cells with the surfaces of these scaffolds *in vitro* under a variety of biochemical and physical conditions at a resolution in the nanometer range.

In a situation that reproduces its natural biological environment, a cell will extend protrusions towards the scaffold. These physical interactions initiate a cascade of events that effect the cytoskeletal organization, signaling pathways, and cell-cell interactions. The initial attachment of the cell with scaffold surface is triggered through a complex interaction of chemical and mechanical receptors at the leading edge of the protrusion. Actin-based cells develop the protrusions through a dynamic cycle of assembly and disassembly of intracelluar actin filaments.. Recent research has provided new insight into the internal signalling cascades that promote the reorganization of actin filaments into aligned and branched internal structures that result in the extension of two different types of protrusions, narrow filopodia and broad

lamellipodia[1, 2]. Surface characteristics that have been demonstrated to effect these actin rearrangements are surface roughness [3], nano-patterning[4], elasticity [5] and curvature [6].

In this work, we evaluate the interaction of the tips of protrusions emanating from NIH 3T3 fibroblasts with 2D planar and 3D nanofibrillar surfaces.

EXPERIMENT

Cell Culture

NIH 3T3 fibroblast cells were cultured for 24 hours on two different surfaces, planar (2D) tissue culture plastic and amine coated nanofibers. The amine coated nanofibers were randomly oriented polyamide nanofibers (a continuous fiber that collects as a nonwoven fabric) electrospun by Donaldson Co., Inc. (Minneapolis, MN). They were electrospun from a blend of two polymers [(C28O4N4H47)n and (C27O4.4N4H50)n] onto plastic coverslips. The polymeric nanofiber mat was crosslinked in the presence of an acid catalyst and formed a dense network of filaments 50-80 nm in diameter with minimal porosity. The nanofibers were covalently coated with a proprietary polyamine polymer by Surmodics, Inc. (Eden Prairie, MN).

Phase Contrast Microscopy

Phase Contrast Microscopy was performed on live cells using an Olmpus 1X70 inverted microscope. The images were captured by using IP lab scientific imaging software.

Cell Fixation and Optical Microscopy

Samples for optical and AFM microscopy were fixed with 2.5% glutaraldehyde in 0.1% phosphate buffer for 15 minutes, briefly rinsed with 0.1M phosphate buffer and washed 3 times with triple distilled water, . The samples were then permitted to desiccate in air for 48 hours prior to optical, AFM and SPRM-AFM imaging. The desiccated samples were optically examined during AFM imaging using a Sony XC-999P CCD color video camera microscope with a VCL-12S12XM lens (f = 12 mm).

SPRM Enhanced Atomic Force Microscopy

Scanning Probe Recognition Microscopy (SPRM) is a new scanning probe microscopy technique developed by our group which allows us to adaptively follow and investigate specific regions of interest using any scanning probe microscopy technique [7, 8] The SPM system itself is given the ability to auto-focus on regions of interest through incorporation of recognition-based tip control. The recognition capability is realized using techniques in pattern recognition and image processing fields. Adaptive learning and prediction are also implemented to make detection and recognition procedures quicker and more reliable. In the present work, SPRM-enhanced atomic force microscopy (SPRM-AFM) was used to investigate the curvature and surface roughness of individual nanofibers, and details of the cell-substrate interfaces.

SPRM is implemented as an adaptation of a Veeco Instruments Nanoscope IIIA system. The system was operated in AFM and SPRM-AFM contact mode in ambient air. Other instrument parameters included the use of a J scanner with a maximum 125x125 square micron x-y scan range and silicon nitride tips with a nominal 20 nm tip radius of curvature.

Experimental Investigation of Cell Response

3T3 NIH fibroblasts are cultured on two different surfaces, tissue culture plastic (2D) and amine coated nanofibers. In order to investigate cell response, fibroblasts cultured on these two surfaces were observed and compared by using different techniques. Phase contrast images of

living fibroblasts at the end of the first 24 hours are shown in figures 1(a) and 2(a). Bright field images of the desiccated cells shown in figures 1(b) and 2(b) show similar morphologies. A difference in cell morphology was observed using phase contrast and bright field microscopy.

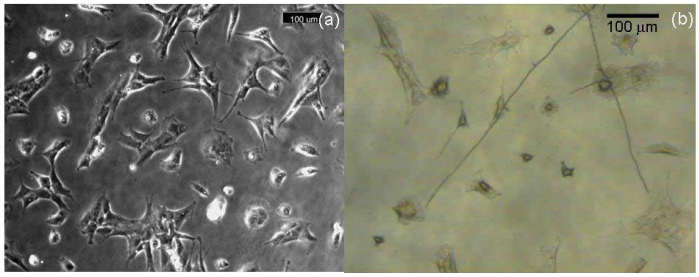

Figure 1. Fibroblasts cultured on 2D surface. (a) Phase contrast microscopy of live cells, and (b) Optical microscopy of fixed cells indicate similar morphologies.

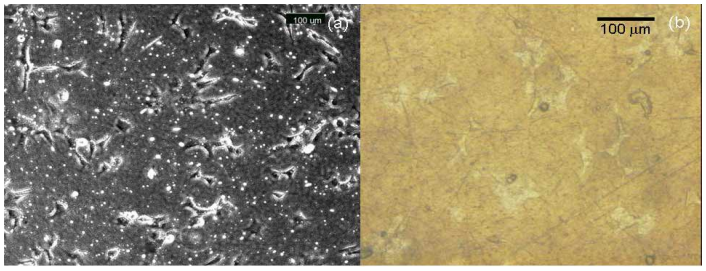

Figure 2. Fibroblasts cultured on amine coated nanofibers. (a) Phase contrast microscopy of live cells, and (b) Optical microscopy of fixed cells indicate similar morphologies.

AFM images shown in figures 3 and 4 provided more detailed information about size, and shape of fibroblasts growing on the two different surfaces. The cell body size of fibroblasts was about 50µm in both cases. However, fibroblasts grown on the tissue culture plastic 2D surface showed fine filopodia-like structures at the ends of pointed projections, as shown in figure 3. Fibroblasts grown on the amine coated nanofibers showed blunted lamellipodia-like projections extending over several nanofibers. These projections lacked the fine filopodia-like end structures. Fibroblasts grown on the amine coated nanofibers were also observed to show a great number of cell-cell interactions between the blunted projections as shown in figure 4. Both factors contributed to the changed appearance of the 2D and nanofiber cultured fibroblasts observed in the images obtained using phase contrast and bright field microscopy.

As previously reported [7], SPRM is able to generate the surface roughness (defined as root mean square) for a local neighborhood region for every pixel on a single nanofiber because of its ability to perform an auto-focused scan that follows within the boundaries of a particular nanofiber. The shape and size of the local neighborhood region can be adjusted, which makes the method adaptable to different samples. For tissue scaffolds, we have experimented with a rectangular box around each pixel approximately on the order of the nanofiber diameter. Multiple sets of overlapping surface roughness information were generated, with the provision that any box that extended outside the nanofiber boundaries was automatically truncated. A surface roughness map along individual nanofibers was then generated. More importantly, a histogram based on data points from the analysis of many individual nanofibers was generated, which allowed the calculation of statistically meaningful surface roughness information, including mode value, mean value variance and shape of the distribution. The surface roughness values for comparable electrospun nanofibers ranged from 0.8~19.7 nm with a variance of 9.1 based on analysis of over 3000 data points.

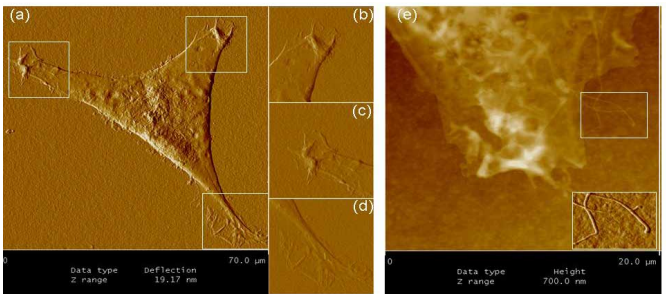

Figure 3. AFM images of 3T3 NIH fibroblast cultured on 2D surface. (a) Deflection image of a typical fibroblast; (b) Close-up deflection image of top right region; (c) Close-up deflection image of top left region; (d) Close-up deflection image of bottom right region; (e) Height image of a projection for another cell showing structures (close-up deflection image in inset).

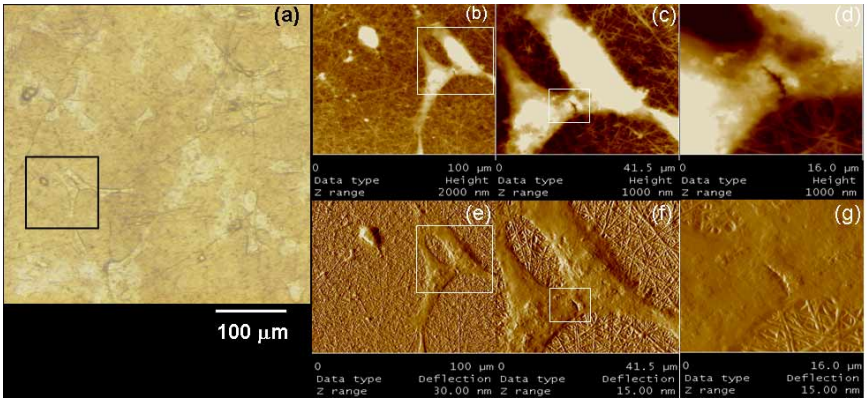

Figure 4. 3T3 NIH fibroblast cultured on amine coated nanofibers. (a) Multiple cell-cell interactions on the amine coated nanofibers are observed in the optical microscopy image. The cells in the black box are shown in close-up AFM images in (b) through (g). (b) through (d): increasing close-up AFM height images; (e) through (g): corresponding increasing close-up AFM deflection images.

Fibroblasts grown on the amine coated nanofibers showed blunted projections extending over multiple nanofibers. Thus, while the surface roughness of the individual nanofibers might be expected to influence cell adhesion, the overall roughness of the nanofiber network may influence cell attachment too. The root mean square surface roughness of a representative 11 square micron area which roughly corresponds to the width of a lamellipodia-like extension was 132 nm.

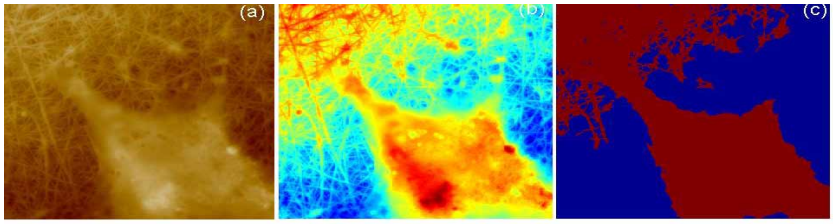

Figure 5. AFM images of 3T3 NIH fibroblast cultured on amine coated nanofibers. Each image is 40 square microns. (a) Height image; (b) Height image with different color map; (c) Detected incorrect cell region using traditional thresholding method.

We are particularly interested in details of the projection regions for the cells. As shown in figure 5 (a), this was indistinct for the cells cultured on nanofibers using conventional AFM

imaging, for all cells examined and for close-up scans (not shown). Traditional thresholding methods based on height information, whether performed by a human observer of the AFM image, or using additional image processing enhancement techniques, could not successfully clarify the cell region at the end of the lamellipodia-like extension. Figures 5 (b) and (c) show the effect of the shadow artifact around main cell body, however, at the region of interest at the end of the lamellipodia-like extension, the height difference is not resolvable.

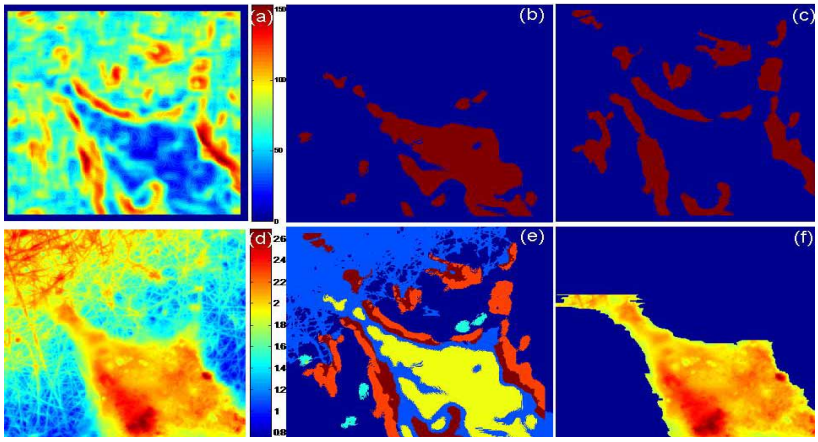

Figure 6. SPRM is used to successfully detect the cell region (a) Roughness map (unit: nm) of the nanofibers mesh; (b) Regions with low roughness below 50nm; (c) Regions with high roughness above 90nm; (d) Original height image (unit: μm); (e) Combination map of height and roughness information; (f) Detected correct cell region.

We have therefore defined a new feature for SPRM-AFM imaging based on the recognition of the surface roughness difference between the nanofiber matrix and the cell surface. The surface roughness map rather than the height image is shown in figure 6 (a). It shows that the cell region has low roughness below 50 nm and the tissue scaffold at the edge of cell has high roughness above 90 nm (we note that the box statistic of 132 nm surface roughness over 11 square microns corresponds to an average of the values shown on the surface roughness amp). This information is important for the successful detection of the cell region. The low roughness region is extracted as shown in figure 6 (b) and the high roughness region is also extracted as shown in figure 6 (c). It is still difficult to accurately identify the cell region based only on difference between these two surface roughness "regions" because they both have noise.

Therefore, a multi-criteria decision rule was designed based on the combination of two types of information: the height information with the surface roughness. The cell region should satisfy the following three criteria: its height is above threshold; it contains the low roughness region indicated by yellow color in figure 6 (e); and it is bounded by the high roughness region indicated by orange color in figure 6(e). By applying these criteria, the cell region can be successfully detected automatically as shown in figure 6 (f). This feature is now under investigation in ongoing SPRM investigations of cell attachment to the nanofiber matrix.

DISCUSSION

NIH 3T3 fibroblasts cultured on two different types of surfaces, tissue culture plastic and amine coated nanofibers, are observed by using phase contrast, bright field, and atomic force microscopy. The cell body size of fibroblasts was about 50μm in both cases. However, fibroblasts grown on the tissue culture plastic 2D surface showed fine filopodia-like structures at

the ends of projections while fibroblasts grown on the amine coated nanofibers showed blunted lamellipodia-like projections extending over multiple nanofibers. Fibroblasts grown on the amine coated nanofibers were also observed to show a greater number of cell-cell interactions between the blunted projections. Both factors contributed to the observed changes in morphology of the fibroblasts cultured on 2D and 3D nanofibrillar surfaces. The appearance of the projections and the greater number of observed cell-cell interactions suggests the possible formation of a greater number of adherens junctions. In a previous report by Nur-E-Kamal et al. [9], it was demonstrated that culture of fibroblasts on nanofibrillar surfaces stimulated the sustained activation of Rac, a small GTPase regulator of cytoskeletal organization and cell mechanics. Since Rac activation is necessary for the formation of adherens junctions [10], it may be speculated that amine-coated nanofibers induce more adherens junction formation by the activation of Rac and its downstream effectors.

CONCLUSIONS

The SPRM system developed by our group enables us to auto-focus on region of interest, such as a single nanofiber or fibroblast for the first time. The new technique makes investigations of tissue scaffold properties directly along individual nanofibers possible. We have investigated curvature and surface roughness properties that have been shown to influence cell attachment in statistically meaningful detail. The fibroblast attachment region of interest can be successfully recognized through the definition of a feature that combines surface roughness information with the height information. This allows us to investigate situations in which traditional AFM height and deflection information is insufficient, which included the lamellipodia-like structures that extended over multiple nanofibers in the current work. SPRM investigations of cell attachment to the 2D and nanoscale 3D nanofibrillar surfaces, and of the observed filopodia-like and lamellipodia-like structures, is continuing.

ACKNOWLEDGEMENTS

The support of National Science Foundation DMI-0400298 is gratefully acknowledged.

REFERENCES

1. T.M. Svitkina and G.G. Borisy, *Lamellipodia. J. Cell Biol.*, **145**, 1009-26 (1999).
2. T.M. Svitkina, E.A. Bulanova, O.Y. Chaga, *J. Cell Biol.*, **160**, 409-21 (2003)
3. D. D. Deligianni, N. D. Katsala, P. G. Koutsoukos, and Y. F. Missirlis, *Biomaterials*, **22**, 87-96 (2001).
4. Matthew John Dalby, Mathis O. Riehle, Duncan S Sutherland, Hossein Agheli, Adam SG Curtis, *Biomaterials*, **25:2323**, 5415-5422 (2004).
5. D. E. Discher, P. Janmey, and Y.-l. Wang, *Science*, **310**, 1139-1143 (2005).
6. Yasuhiro Sawada and Michael P. Sheetz, *J. Cell Biology*, **156**, 609-615 (2002).
7. Y. Fan, Q. Chen, V.M. Ayres, A.D. Baczewski, L. Udpa and S. Kumar, *Int. J. Nanomedicine*, in press.
8. http://www.egr.msu.edu/ebnl, then *Research, Scanning Probe Recognition Microscopy* for an SPRM video demonstration.
9. A. Nur-E-Kamal, I. Ahmed, J. Kamal, M.Schindler, S. Meiners, *Stem Cells* **24** 426-433 (2005)
10. RM Ray, RJ Vaidya, and LR Johnson, *Cell Motil Cytoskeleton* **64** 143-156 (2007)